https://doi.org/10.5194/egusphere-2026-4022
Preprint. Discussion started: 6 August 2026

Long-term evolution of stratospheric water vapor from the Hunga eruption

Kimberlee Dubé[1], William Randel[2], Adam Bourassa[1], Susann Tegtmeier[1], Xinyue Wang[3], Jun Zhang[2], Eilidh Hlady[1], Meghan Brehon[1], Sergey Khaykin[4], and Douglas Degenstein[1]

[1]Institute of Space and Atmospheric Studies, University of Saskatchewan, Saskatoon, SK, Canada
[2]NSF National Center for Atmospheric Research, Boulder, CO, USA
[3]Department of Atmospheric and Oceanic Sciences, University of Colorado Boulder, Boulder, CO, USA
[4]Laboratoire Atmosphère Observations Spatiales, UVSQ, CNRS, Sorbonne Université, Guyancourt, France.

Correspondence: Kimberlee Dubé (kimberlee.dube@usask.ca)

Abstract. The Hunga underwater volcanic eruption in January 2022 injected 150 Tg of water vapour (H_2O) into the stratosphere, increasing the total stratospheric H_2O mass by 10%. This study investigates the transport of the Hunga H_2O within, and out of, the stratosphere from 2022–2025, using H_2O observations from the Microwave Limb Sounder (MLS) and the Atmospheric Chemistry Experiment – Fourier Transform Spectrometer (ACE-FTS), along with model simulations from the Whole Atmosphere Community Climate Model (WACCM) and the FLEXible PARTicle dispersion model (FLEXPART). The Hunga H_2O is isolated by using the tropical cold point temperature to account for H_2O that entered the stratosphere through the tropical tropopause, rather than via the eruption. The resulting residuals show the detailed evolution of the Hunga H_2O over time while it moves to higher latitudes and lower altitudes. Including the lower stratosphere, approximately two-thirds of the Hunga H_2O remains in the stratosphere in late 2025. There is good agreement between the observed and modelled H_2O above 20 km. However, in the lower stratosphere observations show substantially more H_2O compared to the model during 2024 and 2025, suggesting that the modelled transport across the lower stratosphere is too fast. Observations show excess H_2O in the tropics in 2023 and 2024, suggesting evidence of recirculation from SH mid-latitudes back to the tropics. This mixing signature is found in WACCM simulations and confirmed in FLEXPART transport calculations. Including the lower stratosphere in the calculation increases the decay time scale of the Hunga stratospheric water vapor by 1–2 years.

1 Introduction

The Hunga underwater volcano (20.5°S, 175.4°W) erupted on January 13 and 15, 2022. The highest volcanic plume reached the mesosphere, traveling up to an altitude of 58 km (Carr et al., 2022; Proud et al., 2022), while the main volcanic plume detrained at 30–35 km, with rapid descent due to water vapor cooling to ∼25–30 km. Approximately 0.5–1 Tg of SO_2 were injected into the stratosphere (APARC, 2025), along with ∼150 Tg of water vapor (H_2O), corresponding to 10% of the global stratospheric background H_2O mass (Millán et al., 2022; Khaykin et al., 2022; APARC, 2025). While this amount of SO_2 is relatively low, Hunga still resulted in the largest increase in stratospheric aerosol since the 1991 Mount Pinatubo eruption, which injected 15 Tg of SO_2 (Guo et al., 2004). The magnitude of H_2O injected by Hunga is unprecedented in the satellite

https://doi.org/10.5194/egusphere-2026-4022
Preprint. Discussion started: 6 August 2026

era. The excess stratospheric H_2O injected by Hunga contributed to ongoing cooling in the middle and upper stratosphere and warming in the lower stratosphere that persisted until mid-2023, both resulting in circulation changes (Coy et al., 2022; Wang et al., 2023; Fleming et al., 2024; Stocker et al., 2024; Randel et al., 2024). The Hunga H_2O also influenced stratospheric chemistry: it caused rapid sulfate aerosol formation through the production of OH from H_2O (Zhu et al., 2022; Asher et al., 2023), and altered chlorine and nitrogen partitioning, although the impact on ozone at all latitudes was minimal (Zhang et al., 2024b, a; Santee et al., 2023; APARC, 2025; Bednarz et al., 2026).

Typically, H_2O enters the stratosphere through the tropical cold point tropopause, where the cold temperatures limit the amount of moisture by freeze-drying the air (Brewer, 1949). This results in an imprint of seasonal variations in the cold point temperature on stratospheric water vapor, commonly referred to as the "tape recorder" (Mote et al., 1996). A similar process occurs for interannual variations, where water vapor closely follows cold point temperature changes (Randel and Park, 2019). An additional source of stratospheric water vapor that becomes important above ∼10 hPa (∼30 km) is methane (CH_4) oxidation (Jones et al., 1986; Frank et al., 2018). H_2O is mainly removed from the stratosphere through transport to the troposphere in the extratropics by the Brewer-Dobson circulation (BDC) (e.g., Holton et al., 1995; Plumb, 2002), through ice polar stratospheric cloud (PSC) sedimentation in the polar vortex in the presence of low temperatures (e.g., Fahey et al., 1990; Vömel et al., 1995; Jiménez et al., 2006), and ascent to the mesosphere, where H_2O is destroyed by Lyman-alpha photolysis (e.g., Nicolet, 1981).

Given its unique occurrence and significant impacts on stratospheric processes, it is important to determine when and where the Hunga water vapor is exiting the stratosphere. The Hunga H_2O was initially injected into the Southern Hemisphere (SH) tropics, and some of the H_2O had already crossed the equator within a month of the eruption (Schoeberl et al., 2023). Over the course of the following two years, the Hunga water vapor continued to spread throughout the stratosphere as it was transported by the BDC (Millán et al., 2024; Randel et al., 2024). By the time the H_2O reached higher Southern latitudes in late 2022, the Antarctic polar vortex had already formed, preventing the water vapor from reaching the pole before the breakdown of the vortex in November 2022 (Manney et al., 2023). The first substantial loss of Hunga H_2O, by dehydration due to PSC sedimentation in the polar vortex, therefore occurred the following year, in the Antarctic winter and spring of 2023 (Santee et al., 2024; Zhou et al., 2024). Zhou et al. (2024) found that the total amount of H_2O lost in the 2023 vortex was ∼20 Tg. A multi-model assessment of Hunga H_2O evolution (Zhuo et al., 2025) showed reasonable agreement between models and Microwave Limb Sounder (MLS; Waters et al., 2006) observations for global H_2O amounts above 70 hPa (∼19 km) through 2024, and the models project that the total stratospheric water vapor between 1 and 70 hPa will return to background levels between 4 and 7 years after the eruption. The expectation is that the Hunga H_2O will slowly exit the stratosphere mainly via downward transport through the lower stratosphere and across the tropopause in extratropics, although the details of this transport have not been studied.

The goal of our study is to track the transport of the Hunga H_2O within, and out of, the stratosphere during the first 4 years after the eruption, 2022–2025. We use satellite observations from MLS and the Atmospheric Chemistry Experiment - Fourier Transform Spectrometer (ACE-FTS; Bernath et al., 2005). Our analysis domain includes the lowermost stratosphere (LMS; Holton et al., 1995; Appenzeller et al., 1996), down to near-tropopause levels. The extratropical LMS is the region where

https://doi.org/10.5194/egusphere-2026-4022
Preprint. Discussion started: 6 August 2026

stratosphere-troposphere exchange (STE) occurs (Gettelman et al., 2011), and it is in this region that we would expect much of the excess water vapor from the Hunga eruption to exit the stratosphere. The LMS is also important as it is the region where the radiative effects of water vapor are strongest (Solomon et al., 2010; Banerjee et al., 2019). For this work we approximate the LMS as the region between 20 km and the WMO tropopause (WMO, 1957) and the extratropics as latitudes polewards of 30°S and 30°N. We remove interannual variations in H_2O entering the stratosphere linked to tropical cold point temperature (following Randel and Park (2019)) to more clearly focus on the large H_2O variations linked to Hunga. Observations are compared with simulations of Hunga H_2O evolution from the Whole Atmosphere Community Climate Model (WACCM; Gettelman et al., 2019), using free-running ensembles (coupled ocean and fixed sea surface temperature) and a specified dynamics calculation nudged to observed meteorological fields. Aspects of the large-scale H_2O transport are also studied using the FLEXible PARTicle dispersion model (FLEXPART; Bakels et al., 2024).

2 Observations and Models

2.1 MLS

MLS has been in orbit on the Aura spacecraft since July 2004. MLS observes microwave limb emissions and measures approximately 3500 vertical profiles each day between 82°S and 82°N. H_2O is retrieved from observations at 190 GHz (Livesey et al., 2022). The H_2O volume mixing ratio (VMR) profiles have a vertical resolution of ∼3 km from 316–0.22 hPa. Beginning in May 2024, MLS water vapor profiles are only available for ∼6 days each month as the 190 GHz subsystem is otherwise powered off so that its remaining function can be conserved for as long as possible (https://mls.jpl.nasa.gov/, last access: 20 January 2026). We simply bin the data from these reduced observation periods into monthly samples as all latitudes are covered during the measurement period. No MLS observations are available during January 2025.

Version 5 of the MLS retrieval is used here. The data are filtered according to the precision, convergence, and status flags specified by Livesey et al. (2022). However, we do not use the suggested data quality flag threshold of 0.7 that is recommended by Livesey et al. (2022), as Millán et al. (2022) found that most of the early MLS measurements of the Hunga H_2O perturbation do not meet this criterion. Instead, we use a lower data quality flag threshold of 0.1. This allows us to exclude periods of MLS observations with a flag of zero that occurred in 2024, while keeping all the H_2O measurements from directly after the Hunga eruption. A band of enhanced H_2O near 30 km was observed in the v5 MLS observations by Niemeier et al. (2023) and Nedoluha et al. (2024). This is caused by a discontinuity in the a priori used in the MLS retrievals in the 10-8 hPa band (Millán et al., 2024). We account for this by applying the artifact correction described in the supporting information of (Millán et al., 2024)).

While MLS retrievals are performed on a native pressure grid, we chose to perform this study on an altitude grid so that the water vapor in the few kilometers close to the tropopause can be more easily defined. The v5 MLS geopotential height (GPH) profiles that are retrieved along with each H_2O profile are therefore used to convert the H_2O profiles from a pressure grid to a geometric altitude grid. The artifact correction is applied to each MLS profile before converting the profiles from pressure to altitude levels. The final water vapor profiles are then used to calculate the monthly zonal mean H_2O in ten-degree latitude

https://doi.org/10.5194/egusphere-2026-4022
Preprint. Discussion started: 6 August 2026

bins, from 80°S to 80°N. The anomaly is calculated by subtracting the mean H_2O profile from 2005–2021 for each month from the monthly mean H_2O.

2.2 ACE-FTS

ACE-FTS has been in orbit on SCISAT since 2003 and collecting data since February 2004. It is in a high-inclination circular orbit (74°) at 650 km, measuring from 85°S to 85°N. ACE-FTS is an infrared Fourier transform spectrometer, measuring from 750 to 4400 cm^{-1}, with a resolution of 0.02 cm^{-1} (Bernath et al., 2005; Boone et al., 2005). ACE-FTS has a solar occultation viewing geometry, and typically observes 30 occultation events each day, 15 at sunrise and 15 at sunset. Vertical profiles for over 40 molecules and over 20 isotopologues are retrieved from the ACE-FTS measurements (Boone et al., 2020).

The H_2O VMR is retrieved using 54 microwindows between 937 cm^{-1} and 2993 cm^{-1} (Sheese et al., 2017). The resulting profiles extend from 5 to 101 km and have a vertical resolution of 3–4 km. H_2O profiles from version 5.3 of the ACE-FTS retrieval are used here (Boone et al., 2023). All observations are filtered according to the data quality flags developed by Sheese et al. (2015) before any further analysis is performed. 3-month averages are used instead of monthly means so that the full range of latitudes is sampled by each data point. As with MLS, deseasonalized H_2O anomalies are calculated as differences from the corresponding 2005–2021 climatology.

2.3 Tropopause temperature and height

The cold point tropopause (CPT) temperature and the WMO tropopause height are calculated from merged radio occultation (RO) observations (Randel and Starr, 2026). The monthly CPT temperature is smoothed in time with a 1-2-1 filter before doing any further analysis. The WMO tropopause + 2 km is used as the lower bound of the analysis. 2 km is added because of the vertical resolution of the MLS observations (∼3 km), and the desire to exclude tropospheric regions in the analysis.

2.4 WACCM

We use the Community Earth System Model version 2 coupled with the Whole Atmosphere Community Climate Model version 6 (CESM2–WACCM6; Danabasoglu et al., 2020; Gettelman et al., 2019). WACCM6 incorporates comprehensive middle-atmosphere dynamics and interactive chemistry via the MOZART-TS/TSMLT mechanism and simulates aerosols using the MAM4 modal scheme (Liu et al., 2016). The atmospheric component has a horizontal resolution of 0.9° latitude × 1.25° longitude and 70 vertical levels extending to ∼140 km. The simulations span 10 years after the eruption (January 2022-–December 2031) and adopt the CMIP6 SSP2-4.5 emissions scenario (Meinshausen et al., 2020; Zhu et al., 2025; Zhuo et al., 2025). All simulations are initialized from the same atmospheric and oceanic state. For the first 1-2 months of 2022, atmospheric fields are nudged to the MERRA-2 reanalysis (Gelaro et al., 2017) to ensure realistic background conditions at the time of the eruption, after which the model is run in a free-running configuration. Each experiment consists of paired simulations: a "forced" case with an injection of 0.5 Tg SO_2 and 150 Tg H_2O on 15 January, and a corresponding "control" case without the Hunga perturbation. Coupled ocean free running simulations are conducted with interactive ocean and sea ice (FR-WACCM; Zhu et al., 2025). To robustly sample internal variability, each experiment includes 30 ensemble members generated by perturbing the end date of the initial nudging by one day. Model anomalies are defined as the difference between each forced simulations and ensemble-mean control simulation. In addition to the WACCM simulations with the coupled ocean configuration, we consider an ensemble with fixed sea surface temperatures (SST) (30 members with Hunga forcing and 30 control runs). These SSTs are derived from an observation-based climatology and repeat each year over 2022–2031 Zhu et al. (2025). Results from a separate specified dynamics case (so-called WACCM-SD) are also included for Hunga forced and control simulations. In the specified dynamics configuration, the winds and temperature are nudged to MERRA-2; these results are an update to WACCM-SD runs in Zhang et al. (2024b, a). SD runs allow for a more direct comparison with observed atmospheric conditions and helping to isolate the contribution of dynamical variability.

2.5 FLEXPART

Backward trajectory simulations were performed using version 11 of the FLEXible PARTicle (FLEXPART) Lagrangian particle dispersion model (Bakels et al., 2024) driven by hourly ERA5 meteorological fields on a 0.5° latitude x 0.5° longitude grid with 137 vertical levels up to 0.01 hPa (Hersbach et al., 2020). FLEXPART is a stochastic model which calculates trajectories for a large number of particles either forward or backward in time through the simulation of transport (including convection), diffusion, and wet and dry deposition. Here, we use air tracer particles released in the tropical lower stratosphere between 15°S to 15°N in latitude and 18 km to 21.5 km in altitude. 300 000 particles were released throughout December 2023, evenly spaced in time. The backward simulation mode allows for potential source contributions to the region of the tropical lower stratosphere to be determined. The model output gives the position of the simulated air parcels every 3 hours for the simulation period of January to December 2023.

3 Results and Discussion

3.1 Removing H_2O variability tied to the cold point tropical tropopause

The Hunga water vapor anomalies in the LMS can be isolated by accounting for water vapor variations tied to interannual changes of the tropical CPT temperature. This is done using modified calculations from Randel and Park (2019), based on lag regressions of H_2O onto CPT temperature, which can accurately track H_2O interannual changes in the tropical pipe and global lower stratosphere. The calculations are based on deseasonalized monthly mean temperature and H_2O anomalies. The CPT temperature-H_2O lag regressions are trained using the pre-Hunga period (2005–2021) and then extended post-2022 using the observed CPT temperature time series. The calculations determine the time lag τ of the maximum correlation with CPT temperature as a function of latitude ϕ and altitude z to track the vertical and horizontal propagation of the corresponding H_2O anomalies. The observed CPT temperature time series with the appropriate lag is then scaled by the regression slope of H_2O onto the optimally lagged CPT temperature to obtain the reconstructed H_2O anomalies at some time t and location:

$$\mathrm{H_2O_{recon}}(\phi,z,t) = \frac{\Delta \mathrm{H_2O}(\phi,z,t)}{\Delta \mathrm{T_{CP}}(t-\tau)} \times \mathrm{T_{CP}}(t-\tau). \quad (1)$$

https://doi.org/10.5194/egusphere-2026-4022
Preprint. Discussion started: 6 August 2026

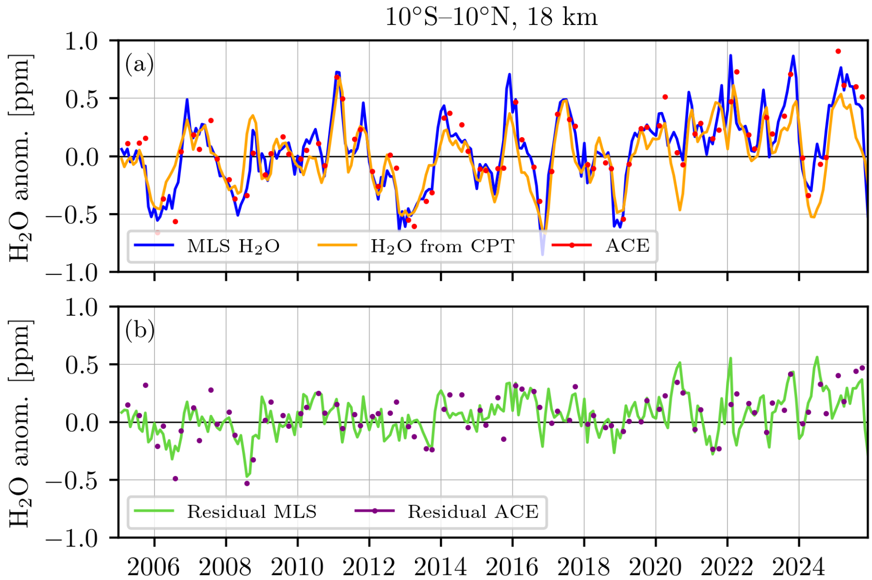

Figure 1. (a) Deseasonalized ACE-FTS and MLS H_2O anomalies and the H_2O anomaly from the cold point temperature reconstruction at 18 km in the tropics. (b) The difference between the observed H_2O anomalies and the H_2O anomaly from the cold point temperature reconstruction.

The result is subsequently referred to as the "cold point reconstructed H_2O" or the "H_2O from CPT", and the difference between this and the observed H_2O is called the residual. Unlike in Randel and Park (2019), the optimal lags are not calculated for each month of the year individually, but rather for all the monthly mean observations in a single latitude/altitude bin, as this was found to result in a smoother reconstructed H_2O time series. The cold point reconstructed H_2O is highly correlated with the observed MLS H_2O within the LMS during the 16-years prior to the Hunga eruption (Appendix Figure A1).

An example of the calculations applied near the location of the CPT (18 km, 10° N–S) is illustrated in Figure 1, showing observed MLS H_2O anomalies together with the corresponding cold point reconstructed H_2O. At this location, the cold point reconstructed H_2O describes most of the variability in the observed H_2O, and the correlation between the two datasets is 0.85. The difference between the two datasets, referred to as the residual H_2O, is less than ± 0.5 ppm until 2020. Larger (positive) residuals are observed after 2020, and these are attributed to the effects of Hunga itself (after 2022), along with H_2O directly injected into the lower stratosphere in early 2020 by the Australian New Year's fires (Khaykin et al., 2020; Randel et al., 2024; Peng et al., 2026).

The sparser ACE-FTS sampling in the tropics prevents the calculation of robust monthly lag-correlation relationships between H_2O and CPT temperature. Instead, the H_2O reconstruction based on MLS H_2O is subtracted from the ACE-FTS observations to derive the residual H_2O for those datasets. Figure 1 shows that both the tropical ACE-FTS anomaly and the residual are very similar to those from MLS. Note that only months with at least 15 ACE-FTS observations between 10°S and 10°N are included in Figure 1. The very good agreement between ACE-FTS and MLS provides confidence in both datasets.

https://doi.org/10.5194/egusphere-2026-4022
Preprint. Discussion started: 6 August 2026

The subsequent analysis is done in terms of the water vapor mass anomaly. For a given 1 km altitude layer, latitude, and month the H_2O mass anomaly is defined as

$$m_{\mathrm{H_2O}}(z,\phi,t) = S(\phi)\frac{M_{\mathrm{H_2O}}}{gM_{\mathrm{air}}}X(z,\phi,t)\left(P(z-0.5\mathrm{km})-P(z+0.5\mathrm{km})\right), \quad (2)$$

where X is the water vapor mixing ratio, g is the acceleration due to gravity (9.81 $\mathrm{ms^{-2}}$), M_{air} is the molar mass of air (28.96 $\mathrm{gmol^{-1}}$), M_{H_2O} is the molar mass of water (18.02 $\mathrm{gmol^{-1}}$), and $P(z-0.5km)$ and $P(z+0.5km)$ are the pressures at altitude z plus or minus half a kilometer. $S(\phi)$ is the surface area of the chosen latitude band. The mass is calculated for 10-degree latitude bands and 1 km altitude layers, which are later summed to get the total mass in various larger regions of the stratosphere.

The near-global monthly mean water vapor mass from 2015–2025 that is expected based on the observed CPT temperature is shown in Figure 2, panel (a). The upward propagating tape recorder signal that originates near the tropopause is prominent up to ∼22 km. The MLS and ACE-FTS observations (panels (b) and (c)) have a similar tape recorder signal prior to 2022, after which the water vapor that was injected by Hunga dominates the mass anomaly. Subtracting the cold point reconstructed H_2O from the observed H_2O results in estimates of H_2O anomalies that exclude the effects of the transport of tropospheric air into the stratosphere through the cold point. These residuals are the basis for further analysis.

Variability in the cold point temperature explains much of the anomaly in lower stratospheric water vapor prior to the Hunga eruption, apart from 2020, when the Australian wildfires added water vapor to the stratosphere by lofting tropospheric air across the tropopause in midlatitudes (Randel et al., 2024) and also by warming the cold point via aerosol radiative heating (Peng et al., 2026). A higher water vapor anomaly is also present in 2022, after the Hunga eruption, but before the H_2O from the eruption moved to lower altitudes. Starting in 2023, the elevated residual H_2O anomaly at lower altitudes is due to the Hunga water vapor that was transported downwards within the BDC. The upward propagating anomalies in the lower stratosphere after 2023 may suggest the recirculation of Hunga H_2O from midlatitudes back into the tropics and entrainment into the tape recorder: this will be explored further in Section 3.3.

When summed over altitude, the total stratospheric H_2O mass anomaly from the Hunga eruption is approximately 150 Tg in 2022 (Figure 3). This anomaly persists in the MLS and ACE-FTS observations until 2024, after which the stratosphere begins to continuously lose Hunga water vapor at a rate of about 25 Tg per year (the total H_2O mass is ∼100 Tg at the end of 2025). The ACE-FTS and MLS observations are very consistent, even with the differences in sampling. We note the difference in our calculations compared to the analyses of Zhuo et al. (2025) and Zhou et al. (2026), who only consider altitudes above ∼19 km (70 hPa) in evaluating total H_2O mass anomalies, and therefore observed an H_2O mass anomaly of ∼80 Tg at the end of 2024.

Figure 3 also includes the H_2O mass anomaly for 30 WACCM coupled ocean simulations and their mean, along with the specified-dynamics WACCM simulation. The H_2O anomaly in the specified-dynamics WACCM simulation has most of the cold point variability removed by default, as both the volcanic and control runs are nudged to the same winds and temperatures. However, it is important to note that the effect of water vapor entry through the cold point tropopause is not removed from the free-running WACCM simulations. H_2O variability due to the CPT temperature can be accounted for in the model simulations

https://doi.org/10.5194/egusphere-2026-4022
Preprint. Discussion started: 6 August 2026

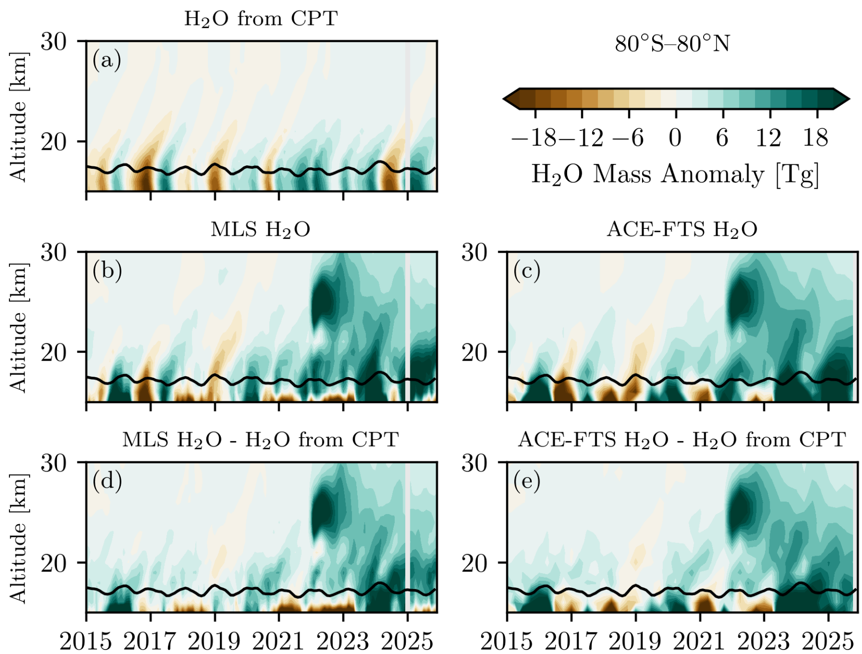

Figure 2. Near global H_2O mass anomaly for (a) the cold point reconstruction (b) MLS observations, (c) ACE-FTS observations, (d) the difference between (a) and (b) (MLS residual), and (e) the difference between (a) and (c) (ACE-FTS residual). MLS is shown as a one-month mean, and ACE-FTS is a 3-month mean. The solid black line denotes the cold point tropopause height. Light gray regions represent missing data.

using the same method as was used for the observations. However, the model results only begin in 2022, and it is necessary to shift the CPT temperature forward in time by the appropriate time lag at each altitude and latitude. This results in missing values in the reconstructed H_2O anomalies near the beginning of the time series, prior to ∼2024 (i.e. if the appropriate time lag for some latitude and altitude in February 2022 is 4-months, there are not any modelled cold point temperatures from 4-months prior that can be used to reconstruct the H_2O). Beginning in 2024, the WACCM ensemble mean changes very little when H_2O variability associated with the CPT temperature is removed, but accounting for H_2O variations due to the CPT temperature can explain some of the variability amongst the individual model realizations, particularly in the tropics (Appendix Figure A2). For these reasons, we do not subtract the CPT reconstructed H_2O from the free-running WACCM simulations in our subsequent analysis.

In Figure 3, the free-running WACCM simulations show that, in the ensemble mean, the global H_2O mass was constant until mid-2023, at which point it dropped by about 20 Tg, likely due to dehydration in the Antarctic winter polar vortex (Zhou et al., 2024). After 2023, the model stratospheric water vapor continued to decrease, with the ensemble mean reaching a value of ∼40 Tg by the end of 2025, which is approaching the range of the typical MLS background variability ($2\sigma = \pm 26$ Tg). The WACCM ensemble mean H_2O anomaly reaches ∼0 Tg by the end of 2028, 6 years after the eruption. The free-running

https://doi.org/10.5194/egusphere-2026-4022
Preprint. Discussion started: 6 August 2026

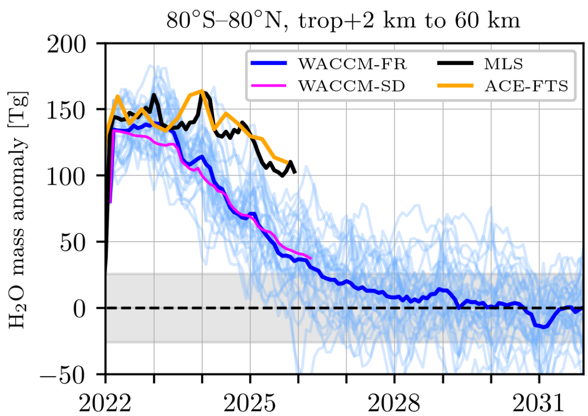

Figure 3. Global mean H_2O mass anomaly from 2 km above the WMO tropopause to 60 km for an ensemble of 30 free-running WACCM simulations, a specified-dynamics WACCM simulation, and the residual water vapor mass from ACE-FTS and MLS. WACCM and MLS are 1-month means, while ACE-FTS is a 3-month mean. Light blue lines represent each individual free-running WACCM realization and the dark blue line is the ensemble mean. The gray shaded region is the 2σ variability in MLS prior to 2022. The observed anomalies are normalized so that the mean in 2021 is zero Tg.

WACCM simulations in Figure 3 use a version of the model that includes a fully coupled ocean. As a comparison, Figure A3 shows the water vapor mass in simulations with fixed SST. There is less variation between the 30 realizations in this version of the model, and the ensemble mean is slightly larger and closer to the observed H_2O mass anomaly. However, this difference is mainly due to a higher H_2O anomaly in 2022 in the fixed SST simulations, and the overall decay rate is comparable in both versions of the model, so the way that the ocean is modeled does not significantly impact our results. The H_2O anomaly from the specified-dynamics WACCM simulation is nearly identical to the free-running ensemble mean, suggesting that the difference between the observations and the model are due to systematic transport biases in WACCM that are not impacted by nudging to observed temperature and wind fields, rather than internal dynamical variability.

The comparisons in Figure 3 show significant differences between satellite observations and WACCM when considering the entire stratosphere. The disagreement between the observed and modelled water vapor mass from mid-2023 onward contrasts with findings from Zhuo et al. (2025) that only considered the H_2O above 70 hPa ($\sim$19 km). Above 70 hPa there is a reasonable agreement between the observed and simulated H_2O mass (shown in Figure 7), so the differences between the observations and the model in Figure 3 are due to variability in the LMS. Calculations of the stratospheric residence time of the Hunga water vapor have thus far neglected the LMS, and projected removal rates may be different when including the entire stratosphere. The differences between the modelled and observed H_2O mass motivates a deeper investigation into the details of the Hunga H_2O in the LMS, which is the main topic of this work.

https://doi.org/10.5194/egusphere-2026-4022
Preprint. Discussion started: 6 August 2026

3.2 Observed and modelled Hunga H_2O evolution and transport through the LMS

We now consider the transport and spread of the Hunga H_2O plume. Figure 4 shows the H_2O mass anomaly evolution during 2022–2025 from ACE-FTS, MLS, and WACCM for annual averages, which highlight the broad-scale evolution. In this and all subsequent Figures the satellite observations are shown in terms of the residual, i.e. H_2O from the CPT reconstruction has been removed. The region between 20 km (dotted black line) and the tropopause+2 km (dashed pink line) is the LMS.

The Hunga H_2O plume was observed over altitudes of ∼20–32 km during most of 2022 (APARC, 2025), extending from SH midlatitudes to just across the equator (∼20°N). Our calculations also show elevated residual H_2O in the LMS during 2022 in both MLS and ACE-FTS data (Figure 4a, 4e), which appears to be from Hunga: Appendix Figure A4 shows the MLS water vapor from 2021/10–2022/9, and the H_2O mass in the LMS increases immediately following the eruption, particularly in the NH. The elevated H_2O in the LMS so soon after the eruption could be from H_2O that detrained between the tropopause and 20 km, from the either the main plume or a separate eruption. By 2023, the satellite data show H_2O transport from the main Hunga plume into the NH midlatitudes above 20 km, and downward transport to lower altitudes in the SH midlatitudes (Figure 4b, 4f). Excess H_2O continues to descend into the LMS in both 2024 and 2025, and both the MLS and ACE-FTS observations show relative maxima in H_2O mass around 18–20 km in both hemispheres in these years.

The WACCM ensemble-mean and WACCM-SD Hunga H_2O evolution is broadly similar to observed behavior, but significantly different in detail, especially in the LMS. Key differences include less model transport into NH midlatitudes above 20 km in 2023 and an absence of extratropical maxima in the model below 20 km after 2023. This produces a very different evolution for the H_2O mass integrated over the entire stratosphere between the model results and observations, as seen in Figure 3. These differences are highlighted in the time versus latitude evolution of the WACCM and MLS H_2O mass integrated above and below 20 km, shown in Figure 5. The observations and model agree qualitatively well above 20 km, although the model shows somewhat less transport into the NH in 2023 and beyond. Variations below 20 km are very different, with much larger amounts of H_2O in the observations. In the model (Figure 5d, 5f), LMS maxima are observed over mid-high latitudes during winter-spring in the respective hemispheres, reflecting the well-known seasonal cycle of downward transport into the LMS via the BDC. Similar LMS seasonal maxima are seen in MLS data (Figure 5b) (and in ACE-FTS data, not shown), but are much larger than in the model ensemble mean. Mixing between mid-latitudes and the tropics is also suggested in the MLS observations (Figure 4d) during the second halves of 2023, 2024, and 2025. The transport in the two WACCM setups is broadly consistent, with the main difference being that the free-running ensemble mean has more H_2O transport to the SH LMS in 2022 and 2023 than the specified-dynamics simulation (Figure 4j, 4n).

Figure 6 provides a complementary perspective on the height vs. time evolution of H_2O anomalies in different latitude bands, spanning polar, midlatitude, and tropical latitudes. Over polar latitudes in the SH (panels e, j, o) there is a distinct seasonal cycle, with enhanced water vapor transport to polar latitudes during the first 6 months of the year, followed by H_2O loss due to PSC dehydration in the winter polar vortex (e.g., Millán et al., 2024; Zhou et al., 2024), which resets the polar H_2O anomaly to near-zero. This did not occur in 2022, as the Hunga H_2O did not reach high latitudes before the formation of the polar vortex (Manney et al., 2023). The total H_2O mass that entered the vortex in 2023 is comparable in WACCM and MLS. In subsequent

https://doi.org/10.5194/egusphere-2026-4022
Preprint. Discussion started: 6 August 2026

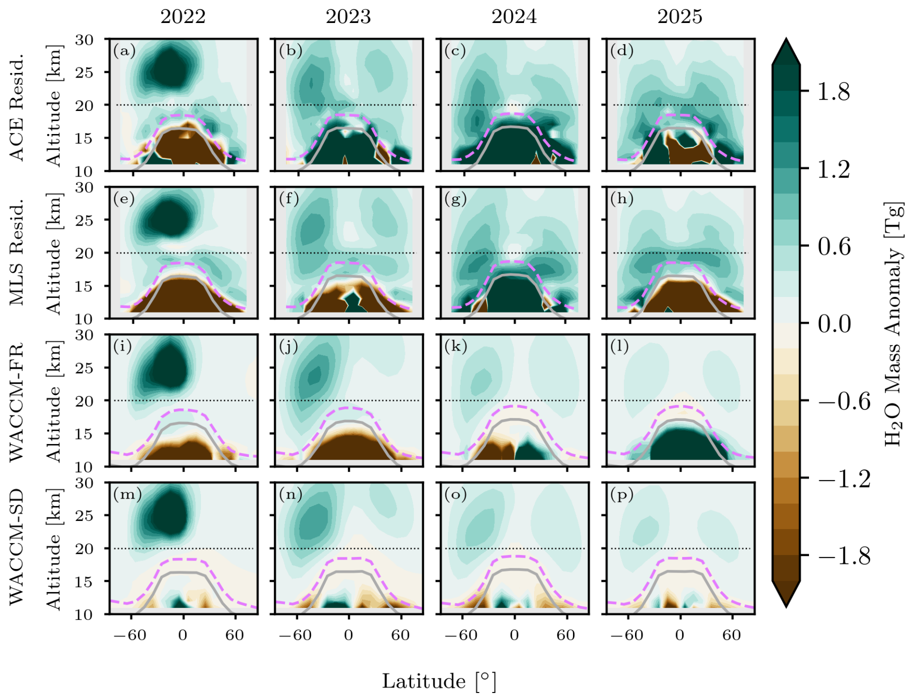

Figure 4. Annual average H_2O mass anomalies during 2022-2025 for the residual water vapor mass in ACE-FTS (panels a-d) and MLS (panels e-h), along with results from the free-running WACCM ensemble mean (panels i-l), and the specified-dynamics WACCM simulation (panels m-p). The sold gray line is the WMO tropopause, and the dashed pink line is the tropopause plus 2 km. The dotted black line at 20 km marks the approximate boundary of the lowermost stratosphere.

years there is less water vapor in the vortex in WACCM, simply because there is less H_2O overall by that point. There is a much smaller seasonal cycle of H_2O in the Arctic (Figure 6a, f, k) because temperatures are typically not cold enough to dehydrate the vortex on a large scale, although this does occur occasionally (Vömel et al., 1997; Khaykin et al., 2013). Zhou et al. (2026) showed that a small amount ($\sim$1 Tg) of dehydration occurred in the Arctic in early 2025. They also found that the weaker and warmer than usual Arctic vortex in the winter of 2023–2024 led to increased descent of Hunga water vapor to the lower stratosphere; this descent is evident in Figure 6a, f, k.

The main features in the mid-latitudes were already apparent in Figure 5. H_2O variability above 20 km is similar in MLS and WACCM, with slow decreases over time. Downward transport into the midlatitude LMS occurs with a seasonal cycle, maximizing during the respective winter-spring seasons, especially clear with the higher H_2O amounts in the SH (Figure 6d, i, n). As noted, MLS has significantly more H_2O mass in the mid-latitude LMS compared to WACCM. Tropical latitudes (30° N-S, Figure 6c, h, m) show the initial Hunga cloud above 20 km that is transported to the extratropics (mostly to the SH) in 2023. At lower levels in the tropics, the MLS data show additional maxima during 2023 and 2024 that propagate upwards with

https://doi.org/10.5194/egusphere-2026-4022
Preprint. Discussion started: 6 August 2026

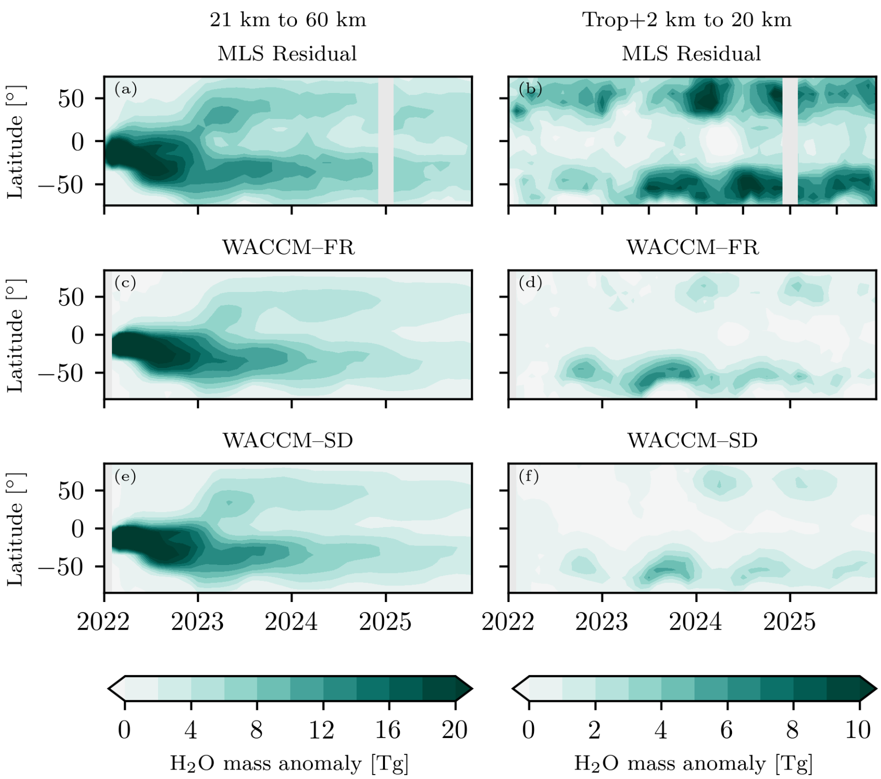

Figure 5. Water vapor mass anomaly for the MLS residual, the free-running WACCM ensemble mean, and the WACCM specified-dynamics simulation above and below 20 km. Light gray regions represent missing data.

time, and some similar (but weaker) behavior is seen in both sets of WACCM results in 2023. This may be evidence of Hunga H_2O that is recirculated from midlatitudes back into the tropics and entrained into the tape recorder, as explored in more detail in Section 3.3.

Finally, we consider the integrated H_2O mass in several regions of the stratosphere to quantify the loss rate of the Hunga H_2O (Figure 7). The individual panels in Figure 7 show the MLS and ACE-FTS results, together with each free-running WACCM realization, the ensemble mean, and the specified-dynamics WACCM simulation. The results are normalized so that the mean anomaly in 2021 is 0 Tg. The H_2O mass anomalies from MLS and ACE-FTS are very similar in each region. By the end of 2025 the MLS H_2O anomaly is $\sim$100 Tg, corresponding to a loss of 50 Tg during the first four years after the eruption. About 50 Tg of the remaining 100 Tg are still in the uppermost stratosphere, while the remaining $\sim$50 Tg have moved to the LMS, with a relatively equal split between the hemispheres. By the end of 2025 the WACCM-FR ensemble mean and the WACCM-SD simulation have anomalies of $\sim$40 Tg of H_2O, most of which is above 20 km. Despite this large difference from the observations in the ensemble mean, some of the model runs are much more comparable to MLS, showing that some of the

https://doi.org/10.5194/egusphere-2026-4022
Preprint. Discussion started: 6 August 2026

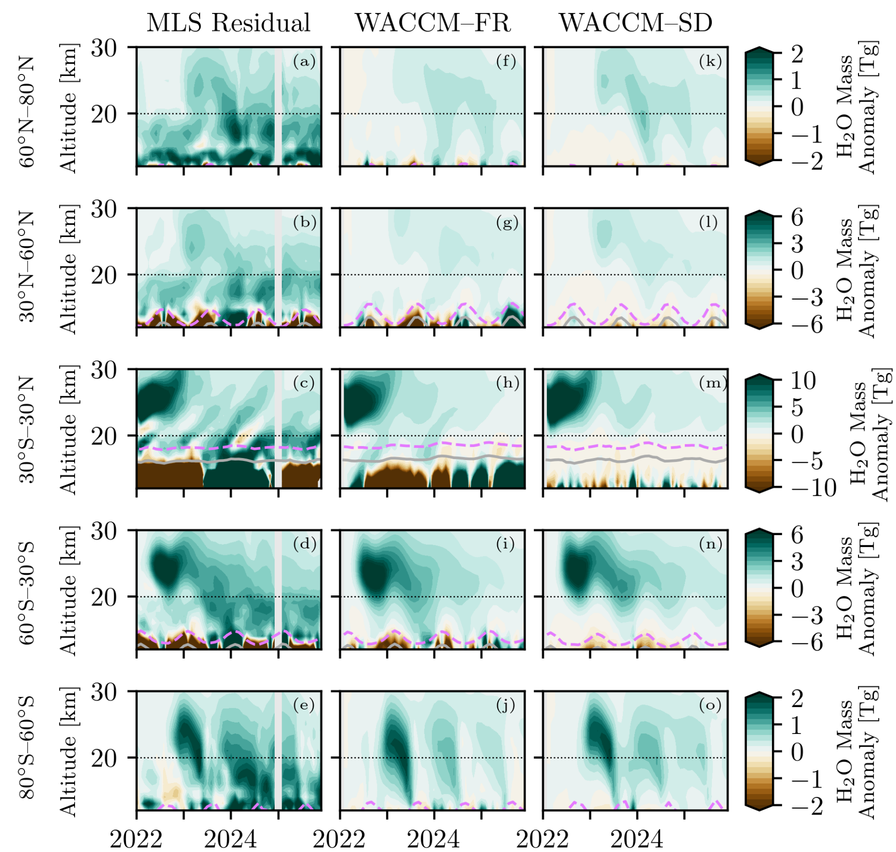

Figure 6. Height vs. time evolution of the water vapor mass anomaly for the MLS residual, the free-running WACCM ensemble mean, and the WACCM specified dynamics simulation in five latitude bands. The sold gray line is the WMO tropopause, and the dashed pink line is the same tropopause plus 2 km. The dotted black line at 20 km marks the approximate boundary of the lowermost stratosphere. Light gray regions represent missing data.

WACCM realizations do compare more favorably with observations, even if the H_2O transport and loss is too fast on average. However, the similarity between the WACCM-SD and WACCM-FR mean H_2O mass anomalies in each region suggests that the differences with the observations are due to systematic issues with the WACCM transport in the LMS rather than some anomalous atmospheric behavior during 2022-2025.

The dark gray shaded region in each panel of Figure 7 is the 2σ range for that bin based on the residual from detrended MLS observations during 2005–2021, and the lighter gray shaded region is the additional 2σ variability in WACCM during 2029–2031. The spread amongst the 30 free-running model simulations is larger than this range in all regions, showing that there is a large uncertainty due to natural variability. In the LMS, the observed H_2O anomaly peaked in 2023 in the model and 2024 in the observations. In the NH LMS (Figure 7d), the observed Hunga signal will no longer be distinguishable from

https://doi.org/10.5194/egusphere-2026-4022
Preprint. Discussion started: 6 August 2026

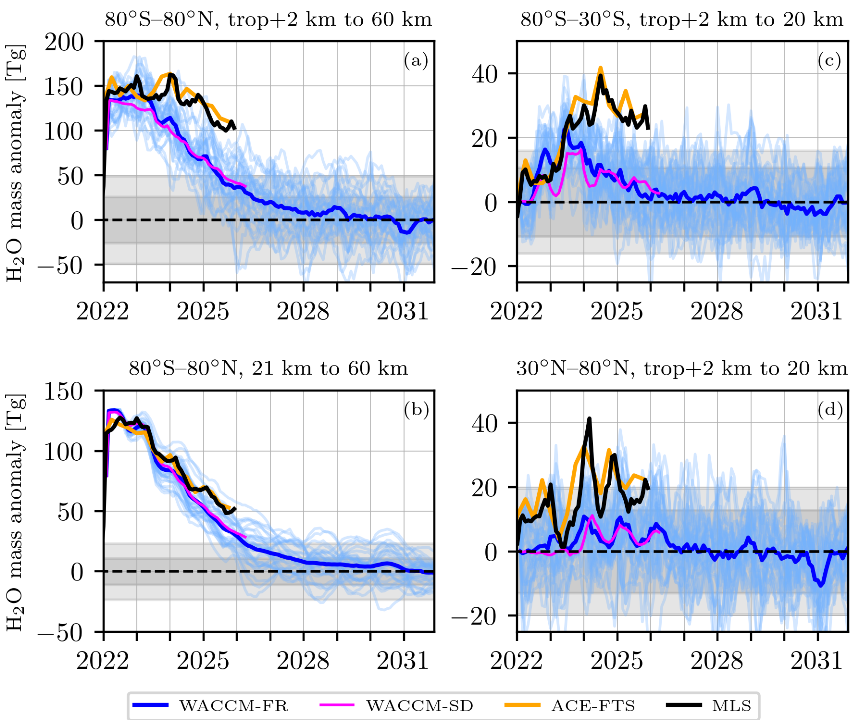

Figure 7. Monthly mean H_2O mass anomaly in several regions for an ensemble of 30 free-running WACCM simulations and the specified-dynamics WACCM simulation, and for the residual water vapor mass from MLS and ACE-FTS (ACE-FTS is a 3-month mean). Light blue lines represent each individual WACCM run. The dark gray shaded region is the 2σ variability in MLS prior to 2022, and the lighter gray shaded region is the additional 2σ variability in WACCM during 2029–2031. The observed anomalies are normalized so that the mean in 2021 is zero Tg.

background variability within 2026, while in the SH LMS (Figure 7c) it may take longer for the Hunga H_2O to become hidden within the background.

The decay rate and the return time of the total Hunga water vapor, as defined by Toohey et al. (2025), are quantified by fitting an exponentially decaying curved to the MLS H_2O mass anomaly. The return time is defined as the number of years since January 2022 needed for the H_2O mass anomaly to be within the 2σ range of the detrended MLS residual during 2005–2021. Figure 8 shows the results with (8a) and without (8b) the inclusion of the LMS. Note that values are provided as a range based on the 2σ uncertainty in the derived rate constant, as the uncertainty in the rate constant does not correspond to a linear change in the decay time scale or return time. When only altitudes above 20 km are considered, the H_2O anomaly begins decreasing at the beginning of 2023, and the decay time scale is [2.80, 3.12] years. Incorporating the LMS increases the decay time scale to [3.32, 4.94] years, and it takes an additional year before the H_2O mass begins to decrease consistently. The return time of the stratosphere to pre-Hunga water vapor levels is [8.00, 10.82] years when the LMS is included in the

https://doi.org/10.5194/egusphere-2026-4022
Preprint. Discussion started: 6 August 2026

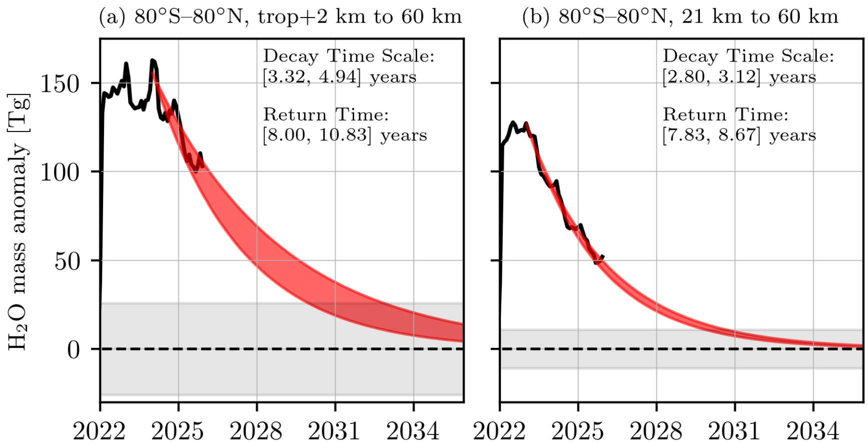

Figure 8. Solid black lines are the near-global monthly mean residual H_2O mass anomaly from MLS for two regions. The gray shaded region is the 2σ variability in MLS prior to 2022. The observed anomalies are normalized so that the mean in 2021 is zero Tg. Red regions are the 2σ range in an exponentially decaying curve fit to the MLS water vapor anomaly beginning in 2024 (panel a) and 2023 (panel b). Decay time scale and return time values are provided as a range based on the 2σ uncertainty in the derived rate constant. Return times are from January 1, 2022.

calculation, which is 1–2 years longer than the return time for H_2O above 20 km. It is also worth noting that the background H_2O variability in the LMS is larger than that at higher altitudes: the 2σ level is 25.89 Tg, compared to 10.92 Tg. The time for the water vapor mass to decay to 10.92 Tg could be as high as 15 years, based on the upper decay time scale for H_2O above trop+2 km.

Earlier studies estimated a return time of 2–10 years (Zhou et al., 2024; Zhuo et al., 2025; Schoeberl et al., 2025). The multi-model study from Zhuo et al. (2025) estimated a return time of 4–7 years, depending on the model, while the most recent estimate based on observations is from Zhou et al. (2026), who found a decay time of 3.36±0.29 years and a return time of 9 years. Our results for water vapor above 20 km are comparable, as our shorter return time is relative to the 2σ background, rather than 1σ background variability used by Zhou et al. (2026) (for a 1σ level, we find a return time of [10.00, 10.50] years above 20 km and [11.00, 12.92] years when the LMS is considered). However, our findings show that earlier studies have likely underestimated the return time for the whole stratosphere by neglecting to consider the LMS.

3.3 Recirculation from midlatitudes back to the tropics

Figures 4, 5, and 6 all suggest that some of the Hunga water vapor is mixed from the mid-latitude LMS back into the tropics and then gets entrained into the tape recorder and recirculated. The most compelling evidence is found in panels (c), (h), and (m) of Figure 6, which show the tropical water vapor anomaly. Both the MLS observations and the WACCM simulations have a tropical water vapor enhancement that begins near the tropopause in mid-2023 and propagates upwards over time. We note that "excess" H_2O near the tropical tropopause during 2023–2024 is also apparent from the time series of MLS H_2O and CPT data in Figure 1. We are confident that this signal is not due to the additional entry of H_2O through the tropopause as it appears in both the observations and the two modelling scenarios, each of which has had the water vapor variability from tropospheric entry removed in a different way.

The monthly mean water vapor mass anomalies for August, October, and December 2023 are provided in Figure 9. In August, there is an elevated H_2O anomaly in the SH LMS (Figure 9a, d). This anomaly appears to move to lower latitudes following the tropopause, reaching the tropics by December (Figure 9c, f). The details and feasibility of this observed in-mixing during 2023 are further examined with back-trajectory simulations from FLEXPART. A set of tracer particles were released just above the tropical tropopause, between 18–22 km and 20°S–20°N, in December 2023. The MLS residual H_2O anomaly in this region was 20.1 Tg in December 2023 (Figure 9c). 17% of the particles that were released in the tropics in December are found to originate from the LMS at SH mid-latitudes (20°S–60°S, 15–20 km) five months earlier, in August 2023, indicating transport and in-mixing of mid-latitude air into the tropics. About 32% of the particles are still in the tropical box in August (Figure 9g) consistent with air masses slowly ascending in the tropical lower stratosphere. Based on the trajectory simulations, we can estimate the amount of Hunga water vapor re-entrained into the tropics. Applying 17% to 20.1 Tg gives 3.4 Tg, suggesting that 3.4 Tg of the 20.1 Tg tropical H_2O anomaly observed in December 2023 is due to transport from the SH LMS. Note that there were already 9.6 Tg of H_2O in the tropical lower stratosphere in August 2023. It is also apparent from the FLEXPART simulation that most of the mixing during July–October is from the SH to the tropics, consistent with the large downward transport of Hunga H_2O in the SH midlatitudes in 2023. These results provide verification that some of the Hunga H_2O that reaches the LMS is not removed from the stratosphere but instead mixes back into the tropics and recirculates. This is further evidence that it cannot be assumed that Hunga water vapor is removed from the stratosphere after passing below 20 km.

4 Conclusions

The 2022 Hunga volcanic eruption injected an unprecedented amount of H_2O into the stratosphere. The transit of the Hunga water vapor through, and subsequently out of, the stratosphere can be tracked using observations from the satellite instruments MLS and ACE-FTS and simulated with a global chemistry-climate model. The Hunga water vapor signal in the LMS was isolated in the observations by subtracting variability associated with changes in the tropical cold point temperature. There is excellent agreement between the residual H_2O anomalies from MLS and ACE-FTS. Both datasets show that the Hunga water vapor had spread to mid- and high latitudes in each hemisphere by 2023, and that approximately 50 Tg of the initial 150 Tg of injected H_2O had been removed from the stratosphere by the end of 2025.

The satellite observations were compared to an ensemble of 30 free-running WACCM simulations and a specified-dynamics WACCM simulation. The observed H_2O decay in the free-running ensemble mean is consistent with that from the observations above 20 km, as has been demonstrated by Zhu et al. (2025). However, on average the modelled H_2O decays much more quickly compared to observations when the LMS is also considered: by the end of 2025 the remaining Hunga H_2O anomaly in MLS and ACE-FTS data is twice as large as the mean WACCM H_2O anomaly. WACCM also has significantly less transport of the Hunga water vapor from the SH to the NH compared to the observations (Figure 5). The specified-dynamics WACCM

https://doi.org/10.5194/egusphere-2026-4022
Preprint. Discussion started: 6 August 2026

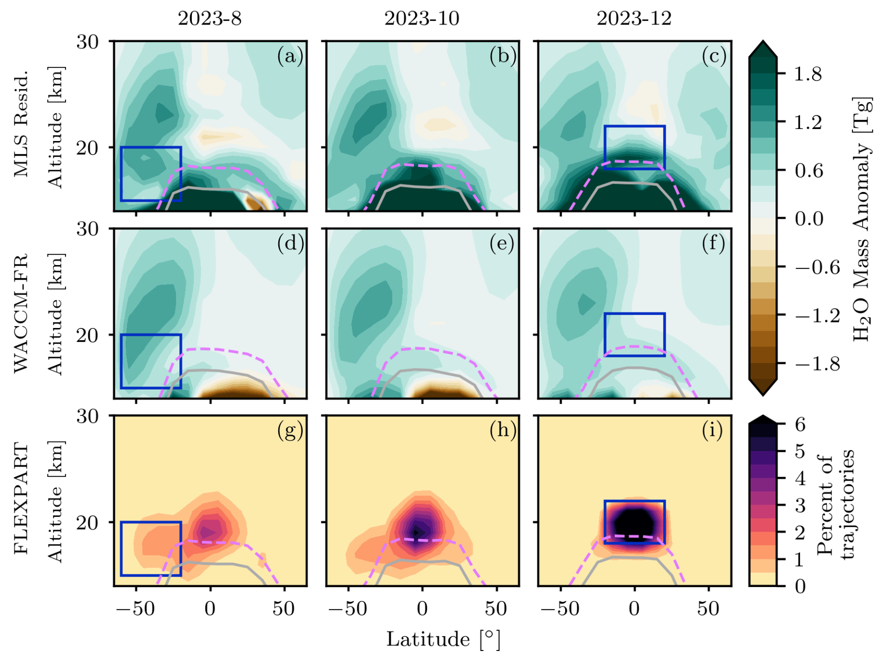

Figure 9. Panels (a)–(c): Monthly mean residual MLS H_2O mass anomaly. Panels (d)–(f): Monthly free-running ensemble mean WACCM H_2O mass anomaly. Panels (g)–(i): average percent of FLEXPART particles in each bin during a given month. The dark blue box in panels (c), (f), and (i) is the particle release box. The dark blue box in panels (a), (d), and (g) is approximately the SH LMS. The solid gray line is the WMO tropopause, and the dashed pink line is the same tropopause plus 2 km.

simulation shows the same water vapor transport as the mean of the free-running simulations, suggesting that the bias with the observations is due to systematic issues with the model transport in the LMS, and not from unusual meteorological variability during 2022–2025.

MLS, ACE-FTS, and WACCM all show evidence that some of the Hunga H_2O is recirculating, rather than being removed from the stratosphere after it passes below 20 km. Trajectory simulations show that approximately 17% of the H_2O that was in the SH LMS in July 2023 had been transported to the tropics 5 months later. However, in reality it is difficult to determine exactly how much of the tropical water vapor anomaly is due to recirculation compared to other sources. Although variability due to water vapor entry via the tropical cold point should be removed, there are associated uncertainties in the calculations, and the entry of tropospheric water vapor could be contributing to the recirculation signal. Nonetheless, the FLEXPART simulations provide evidence that not all Hunga water vapor is removed from the stratosphere after passing below 20 km.

In conclusion, we show that when the LMS is also considered, there is still 100 Tg of Hunga H_2O in the stratosphere compared to 2021 levels at the end of 2025, four years after the eruption. Approximately 20 Tg of the 50 Tg that were lost were removed by Antarctic sedimentation in 2023 (Zhou et al., 2024). Half of the remaining water vapor is in the LMS, below 20 km. Water vapor in the LMS is of particular importance, as this is where the radiative effects of H_2O are greatest, and

https://doi.org/10.5194/egusphere-2026-4022
Preprint. Discussion started: 6 August 2026

so lingering Hunga water vapor in this region is important to quantify. Based on the decay rate of the MLS observations in 2024 and 2025, the total stratospheric water vapor mass will likely return to the level of background variability sometime from 2030 to 2033. These results provide insight into stratospheric transport more broadly, by using the Hunga H_2O to demonstrate transport within the BDC, recirculation, and STE.

Code and data availability.

- MLS v5 geopotential heights are available from Schwartz et al. (2020).
- MLS H_2O volume mixing ratio profiles are available from Lambert et al. (2020).
- MLS diagnostics required for the artifact correction are available from Livesey and Read (2020).
- The observed lapse rate and cold point tropopause are available from Randel and Starr (2026).
- ACE-FTS data are available by registering at https://databace.scisat.ca/level2/ (ACE-FTS, 2026). The data quality flags are available from Sheese and Walker (2025).
- WACCM is a component of the Community Earth System Model (CESM), whose source code is openly available through the CESM GitHub repository: https://github.com/ESCOMP/CESM. CESM2/WACCM6 was developed with support primarily from the National Science Foundation. See Gettelman et al. (2019).
- WACCM results are archived on JASMIN, the UK's collaborative data analysis environment (https://www.jasmin.ac.uk). They are publicly available but require a JASMIN account for access. The data are archived under /gws/nopw/j04/htmip.
- FLEXPART code is available from https://gitlab.phaidra.org/flexpart/flexpart. Documentation is available at https://www.flexpart.eu/ (Bakels et al., 2024).

https://doi.org/10.5194/egusphere-2026-4022
Preprint. Discussion started: 6 August 2026

Appendix A: Additional figures

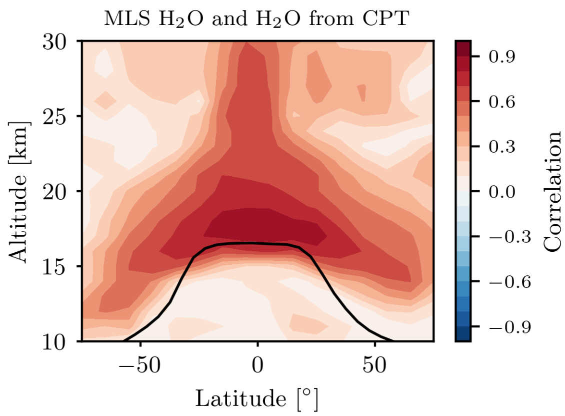

Figure A1. Correlation between MLS H_2O and H_2O reconstructed from the observed cold point temperature for 2005–2021. The solid black line is the mean lapse rate tropopause location.

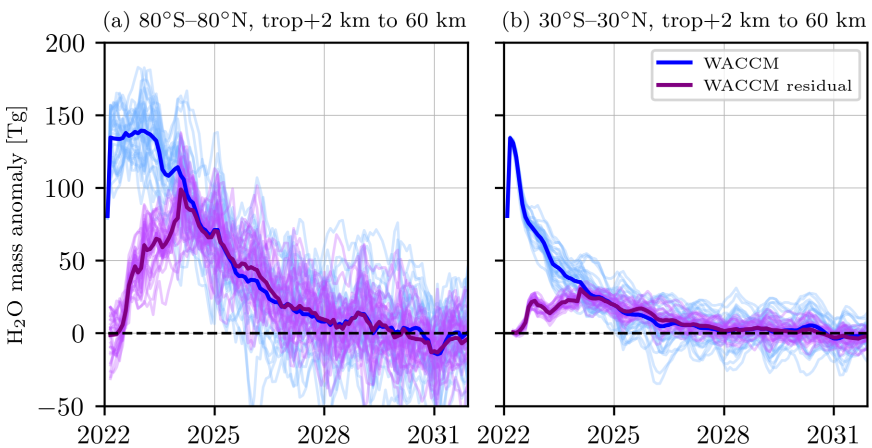

Figure A2. Monthly mean H_2O mass anomaly in two latitudes regions for an ensemble of 30 WACCM realizations. Light blue and purple lines represent each individual WACCM run. Purple lines correspond to WACCM H_2O that has had the variability due to the CPT removed.

https://doi.org/10.5194/egusphere-2026-4022
Preprint. Discussion started: 6 August 2026

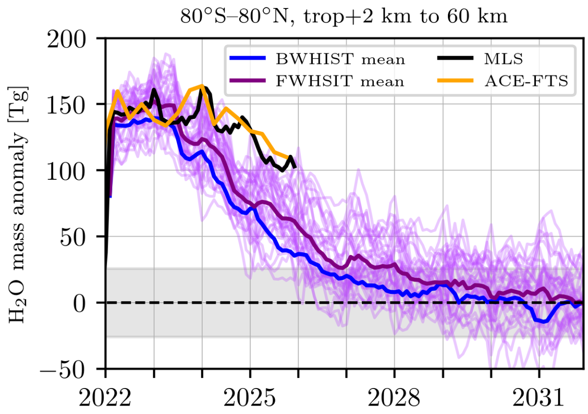

Figure A3. Light purple lines show global mean H_2O mass anomaly from 2 km above the WMO tropopause to 60 km for ensembles of 30 WACCM simulations with Fixed SST (FWHIST). Dark purple is the ensemble mean. Blue line shows the ensemble mean for the fully coupled ocean simulations (BWHIST), the same as in Fig. 3. The residual water vapor mass from ACE-FTS and MLS are also shown. WACCM and MLS are 1-month means, while ACE-FTS is a 3-month mean. The gray shaded region is the 2σ variability in MLS prior to 2022. The observed anomalies are normalized so that the mean in 2021 is zero Tg.

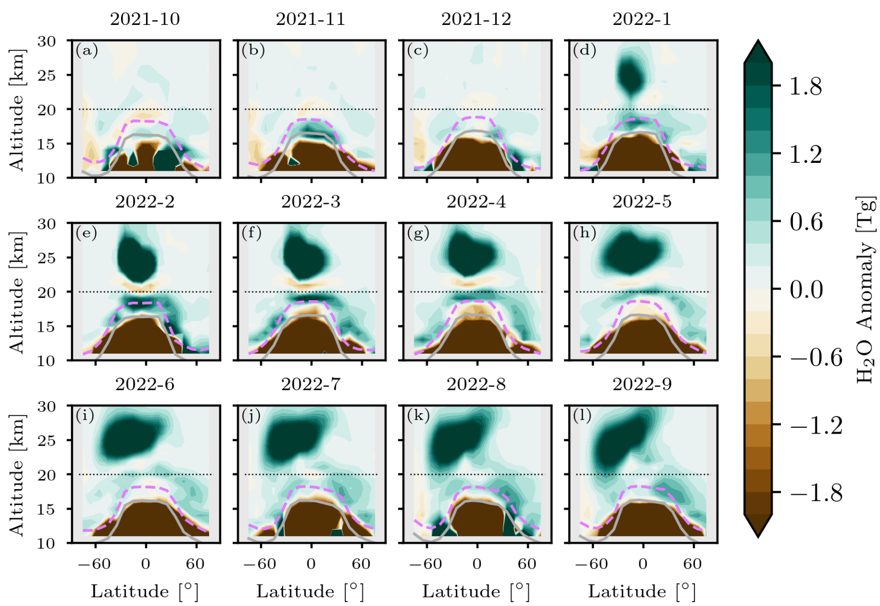

Figure A4. Monthly mean H_2O mass anomalies during 2021/10–2022/9 for the residual water vapor mass in MLS. The sold gray line is the WMO tropopause, and the dashed pink line is the tropopause plus 2 km. The dotted black line at 20 km marks the approximate boundary of the lowermost stratosphere. The large Hunga anomaly beginning in January 2022 is mostly above 20 km, but step-like increases below 20 km are also observed that persist throughout 2022.

Author contributions. KD and WR conceptualized the study and prepared the manuscript. KD conducted the analysis, with contributions from EH. MB conducted the FLEXPART simulations. XW and JZ conducted the WACCM simulations. AB and ST supervised the project. All authors provided significant feedback on the methods and the final manuscript.

Competing interests. We declare that none of the authors has any competing interests.

Acknowledgements. This material is based upon work supported by the NSF National Center for Atmospheric Research, which is a major facility sponsored by the U.S. National Science Foundation under Cooperative Agreement No. 1852977. NCAR's Community Earth System Model project is supported primarily by the National Science Foundation. Computing and data storage resources, including the Derecho supercomputer (doi:10.5065/qx9a-pg09), were provided by the Computational and Information Systems Laboratory (CISL) at NCAR.

References

APARC: The Hunga Volcanic Eruption Atmospheric Impacts Reports, in: APARC Report No. 11, WCRP-10/2025, edited by Zhu, Y., Mann, G., Newman, P. A., and Randel, W., APARC, https://doi.org/10.34734/FZJ-2025-05237, 2025.

Appenzeller, C., Holton, J. R., and Rosenlof, K. H.: Seasonal variation of mass transport across the tropopause, Journal of Geophysical Research: Atmospheres, 101, 15 071–15 078, https://doi.org/https://doi.org/10.1029/96JD00821, 1996.

Asher, E., Todt, M., Rosenlof, K., Thornberry, T., Gao, R.-S., Taha, G., Walter, P., Alvarez, S., Flynn, J., Davis, S. M., Evan, S., Brioude, J., Metzger, J.-M., Hurst, D. F., Hall, E., and Xiong, K.: Unexpectedly rapid aerosol formation in the Hunga Tonga plume, Proceedings of the National Academy of Sciences, 120, e2219547 120, https://doi.org/10.1073/pnas.2219547120, 2023.

Bakels, L., Tatsii, D., Tipka, A., Thompson, R., Dütsch, M., Blaschek, M., Seibert, P., Baier, K., Bucci, S., Cassiani, M., et al.: FLEXPART version 11: Improved accuracy, efficiency, and flexibility, Geoscientific Model Development, 17, 7595–7627, 2024.

Banerjee, A., Chiodo, G., Previdi, M., Ponater, M., Conley, A. J., and Polvani, L. M.: Stratospheric water vapor: an important climate feedback, Climate Dynamics, p. 1697–1710, https://doi.org/https://doi.org/10.1007/s00382-019-04721-4, 2019.

Bednarz, E. M., Butler, A. H., Wang, X., Zhuo, Z., Yu, W., Stenchikov, G., Toohey, M., and Zhu, Y.: Indirect climate impacts of the Hunga eruption, Atmospheric Chemistry and Physics, 26, 197–215, https://doi.org/10.5194/acp-26-197-2026, 2026.

Bernath, P. F., McElroy, C. T., Abrams, M. C., Boone, C. D., Butler, M., Camy-Peyret, C., Carleer, M., Clerbaux, C., Coheur, P.-F., Colin, R., DeCola, P., DeMazière, M., Drummond, J. R., Dufour, D., Evans, W. F. J., Fast, H., Fussen, D., Gilbert, K., Jennings, D. E., Llewellyn, E. J., Lowe, R. P., Mahieu, E., McConnell, J. C., McHugh, M., McLeod, S. D., Michaud, R., Midwinter, C., Nassar, R., Nichitiu, F., Nowlan, C., Rinsland, C. P., Rochon, Y. J., Rowlands, N., Semeniuk, K., Simon, P., Skelton, R., Sloan, J. J., Soucy, M.-A., Strong, K., Tremblay, P., Turnbull, D., Walker, K. A., Walkty, I., Wardle, D. A., Wehrle, V., Zander, R., and Zou, J.: Atmospheric Chemistry Experiment (ACE): Mission overview, Geophysical Research Letters, 32, https://doi.org/https://doi.org/10.1029/2005GL022386, 2005.

Boone, C., Bernath, P., Cok, D., S.C., J., and Steffen, J.: Version 4 retrievals for the atmospheric chemistry experiment Fourier transform spectrometer (ACE-FTS) and imagers, Journal of Quantitative Spectroscopy and Radiative Transfer, 247, 106 939, https://doi.org/https://doi.org/10.1016/j.jqsrt.2020.106939, 2020.

Boone, C., Bernath, P., and Lecours, M.: Version 5 retrievals for ACE-FTS and ACE-imagers, Journal of Quantitative Spectroscopy and Radiative Transfer, 310, 108 749, https://doi.org/https://doi.org/10.1016/j.jqsrt.2023.108749, 2023.

Boone, C. D., Nassar, R., Walker, K. A., Rochon, Y., McLeod, S. D., Rinsland, C. P., and Bernath, P. F.: Retrievals for the Atmospheric Chemistry Experiment Fourier-Transform Spectrometer, Appl. Opt., 44, 7218–7231, https://doi.org/10.1364/AO.44.007218, 2005.

Brewer, A. W.: Evidence for a world circulation provided by the measurements of helium and water vapour distribution in the stratosphere, Quarterly Journal of the Royal Meteorological Society, 75, 351–363, https://doi.org/https://doi.org/10.1002/qj.49707532603, 1949.

Carr, J. L., Horváth, A., Wu, D. L., and Friberg, M. D.: Stereo Plume Height and Motion Retrievals for the Record-Setting Hunga Tonga-Hunga Ha'apai Eruption of 15 January 2022, Geophysical Research Letters, 49, e2022GL098 131, https://doi.org/https://doi.org/10.1029/2022GL098131, 2022.

Coy, L., Newman, P. A., Wargan, K., Partyka, G., Strahan, S. E., and Pawson, S.: Stratospheric Circulation Changes Associated With the Hunga Tonga-Hunga Ha'apai Eruption, Geophysical Research Letters, 49, e2022GL100 982, https://doi.org/https://doi.org/10.1029/2022GL100982, 2022.

Danabasoglu, G., Lamarque, J.-F., Bacmeister, J., Bailey, D. A., DuVivier, A. K., Edwards, J., Emmons, L. K., Fasullo, J., Garcia, R., Gettelman, A., Hannay, C., Holland, M. M., Large, W. G., Lauritzen, P. H., Lawrence, D. M., Lenaerts, J. T. M., Lindsay, K., Lipscomb,

https://doi.org/10.5194/egusphere-2026-4022
Preprint. Discussion started: 6 August 2026

W. H., Mills, M. J., Neale, R., Oleson, K. W., Otto-Bliesner, B., Phillips, A. S., Sacks, W., Tilmes, S., van Kampenhout, L., Vertenstein, M., Bertini, A., Dennis, J., Deser, C., Fischer, C., Fox-Kemper, B., Kay, J. E., Kinnison, D., Kushner, P. J., Larson, V. E., Long, M. C., Mickelson, S., Moore, J. K., Nienhouse, E., Polvani, L., Rasch, P. J., and Strand, W. G.: The Community Earth System Model Version 2 (CESM2), Journal of Advances in Modeling Earth Systems, 12, e2019MS001 916, https://doi.org/https://doi.org/10.1029/2019MS001916, 2020.

Fahey, D., Kelly, K., Kawa, S., Tuck, A., Loewenstein, M., Chan, K., and Heidt, L.: Observations of denitrification and dehydration in the winter polar stratospheres, Nature, 344, 321–324, https://doi.org/https://doi.org/10.1038/344321a0, 1990.

Fleming, E. L., Newman, P. A., Liang, Q., and Oman, L. D.: Stratospheric Temperature and Ozone Impacts of the Hunga Tonga-Hunga Ha'apai Water Vapor Injection, Journal of Geophysical Research: Atmospheres, 129, e2023JD039 298, https://doi.org/https://doi.org/10.1029/2023JD039298, 2024.

Frank, F., Jöckel, P., Gromov, S., and Dameris, M.: Investigating the yield of H_2O and H_2 from methane oxidation in the stratosphere, Atmospheric Chemistry and Physics, 18, 9955–9973, https://doi.org/10.5194/acp-18-9955-2018, 2018.

Gelaro, R., McCarty, W., Suárez, M. J., Todling, R., Molod, A., Takacs, L., Randles, C. A., Darmenov, A., Bosilovich, M. G., Reichle, R., Wargan, K., Coy, L., Cullather, R., Draper, C., Akella, S., Buchard, V., Conaty, A., da Silva, A. M., Gu, W., Kim, G.-K., Koster, R., Lucchesi, R., Merkova, D., Nielsen, J. E., Partyka, G., Pawson, S., Putman, W., Rienecker, M., Schubert, S. D., Sienkiewicz, M., and Zhao, B.: The Modern-Era Retrospective Analysis for Research and Applications, Version 2 (MERRA-2), Journal of Climate, 30, 5419 – 5454, https://doi.org/10.1175/JCLI-D-16-0758.1, 2017.

Gettelman, A., Hoor, P., Pan, L. L., Randel, W. J., Hegglin, M. I., and Birner, T.: The extratropical upper troposphere and lower stratosphere, Reviews of Geophysics, 49, https://doi.org/https://doi.org/10.1029/2011RG000355, 2011.

Gettelman, A., Mills, M. J., Kinnison, D. E., Garcia, R. R., Smith, A. K., Marsh, D. R., Tilmes, S., Vitt, F., Bardeen, C. G., McInerny, J., Liu, H.-L., Solomon, S. C., Polvani, L. M., Emmons, L. K., Lamarque, J.-F., Richter, J. H., Glanville, A. S., Bacmeister, J. T., Phillips, A. S., Neale, R. B., Simpson, I. R., DuVivier, A. K., Hodzic, A., and Randel, W. J.: The Whole Atmosphere Community Climate Model Version 6 (WACCM6), Journal of Geophysical Research: Atmospheres, 124, 12 380–12 403, https://doi.org/https://doi.org/10.1029/2019JD030943, 2019.

Guo, S., Bluth, G. J. S., Rose, W. I., Watson, I. M., and Prata, A. J.: Re-evaluation of SO2 release of the 15 June 1991 Pinatubo eruption using ultraviolet and infrared satellite sensors, Geochemistry, Geophysics, Geosystems, 5, https://doi.org/https://doi.org/10.1029/2003GC000654, 2004.

Hersbach, H., Bell, B., Berrisford, P., Hirahara, S., Horányi, A., Muñoz-Sabater, J., Nicolas, J., Peubey, C., Radu, R., Schepers, D., et al.: The ERA5 global reanalysis, Quarterly journal of the royal meteorological society, 146, 1999–2049, 2020.

Holton, J. R., Haynes, P. H., McIntyre, M. E., Douglass, A. R., Rood, R. B., and Pfister, L.: Stratosphere-troposphere exchange, Reviews of Geophysics, 33, 403–439, https://doi.org/https://doi.org/10.1029/95RG02097, 1995.

Jiménez, C., Pumphrey, H. C., MacKenzie, I. A., Manney, G. L., Santee, M. L., Schwartz, M. J., Harwood, R. S., and Waters, J. W.: EOS MLS observations of dehydration in the 2004–2005 polar winters, Geophysical Research Letters, 33, https://doi.org/https://doi.org/10.1029/2006GL025926, 2006.

Jones, R., Pyle, J., Harries, J., Zavody, A., Russell III, J., and Gille, J.: The water vapour budget of the stratosphere studied using LIMS and SAMS satellite data, Quarterly Journal of the Royal Meteorological Society, 112, 1127–1143, https://doi.org/https://doi.org/10.1002/qj.49711247412, 1986.

https://doi.org/10.5194/egusphere-2026-4022
Preprint. Discussion started: 6 August 2026

Khaykin, S., Legras, B., Bucci, S., Sellitto, P., Isaksen, L., Tencé, F., Bekki, S., Bourassa, A., Rieger, L., Zawada, D., et al.: The 2019/20 Australian wildfires generated a persistent smoke-charged vortex rising up to 35 km altitude, Communications Earth & Environment, 1, 22, https://doi.org/https://doi.org/10.1038/s43247-020-00022-5, 2020.

Khaykin, S., Podglajen, A., Ploeger, F., Grooß, J.-U., Tence, F., Bekki, S., Khlopenkov, K., Bedka, K., Rieger, L., Baron, A., Godin-Beekmann, S., Legras, B., Sellitto, P., Sakai, T., Barnes, J., Uchino, O., Morino, I., Nagai, T., Wing, R., Baumgarten, G., Gerding, M., Duflot, V., Payen, G., Jumelet, J., Querel, R., Liley, B., Bourassa, A., Clouser, B., Feofilov, A., Hauchecorne, A., and Ravetta, F.: Global perturbation of stratospheric water and aerosol burden by Hunga eruption, Communications Earth & Environment, 3, https://doi.org/10.1038/s43247-022-00652-x, 2022.

Khaykin, S. M., Engel, I., Vömel, H., Formanyuk, I. M., Kivi, R., Korshunov, L. I., Krämer, M., Lykov, A. D., Meier, S., Naebert, T., Pitts, M. C., Santee, M. L., Spelten, N., Wienhold, F. G., Yushkov, V. A., and Peter, T.: Arctic stratospheric dehydration – Part 1: Unprecedented observation of vertical redistribution of water, Atmospheric Chemistry and Physics, 13, 11 503–11 517, https://doi.org/10.5194/acp-13-11503-2013, 2013.

Liu, X., Ma, P.-L., Wang, H., Tilmes, S., Singh, B., Easter, R. C., Ghan, S. J., and Rasch, P. J.: Description and evaluation of a new four-mode version of the Modal Aerosol Module (MAM4) within version 5.3 of the Community Atmosphere Model, Geoscientific Model Development, 9, 505–522, https://doi.org/10.5194/gmd-9-505-2016, 2016.

Livesey, N. J., Read, W. G., Wagner, P. A., Froidevaux, L., Santee, M. L., Schwartz, M. J., Lambert, A., Millán Valle, L. F., Pumphrey, H. C., Manney, G. L., Fuller, R. A., Jarnot, R. F., Knosp, B. W., and Lay, R. R.: Aura Microwave Limb Sounder (MLS) Version 5.0x Level 2 and 3 data quality and description document., Tech. Rep. JPL D-105336 Rev. B, Jet Propulsion Laboratory, California Institute of Technology, Pasadena, California, 91109-8099, 2022.

Manney, G. L., Santee, M. L., Lambert, A., Millán, L. F., Minschwaner, K., Werner, F., Lawrence, Z. D., Read, W. G., Livesey, N. J., and Wang, T.: Siege in the Southern Stratosphere: Hunga Tonga-Hunga Ha'apai Water Vapor Excluded From the 2022 Antarctic Polar Vortex, Geophysical Research Letters, 50, e2023GL103 855, https://doi.org/https://doi.org/10.1029/2023GL103855, 2023.

Meinshausen, M., Nicholls, Z. R. J., Lewis, J., Gidden, M. J., Vogel, E., Freund, M., Beyerle, U., Gessner, C., Nauels, A., Bauer, N., Canadell, J. G., Daniel, J. S., John, A., Krummel, P. B., Luderer, G., Meinshausen, N., Montzka, S. A., Rayner, P. J., Reimann, S., Smith, S. J., van den Berg, M., Velders, G. J. M., Vollmer, M. K., and Wang, R. H. J.: The shared socio-economic pathway (SSP) greenhouse gas concentrations and their extensions to 2500, Geoscientific Model Development, 13, 3571–3605, https://doi.org/10.5194/gmd-13-3571-2020, 2020.

Millán, L., Santee, M. L., Lambert, A., Livesey, N. J., Werner, F., Schwartz, M. J., Pumphrey, H. C., Manney, G. L., Wang, Y., Su, H., Wu, L., Read, W. G., and Froidevaux, L.: The Hunga Tonga-Hunga Ha'apai hydration of the stratosphere, Geophysical Research Letters, 49, https://doi.org/10.1029/2022gl099381, 2022.

Millán, L., Read, W. G., Santee, M. L., Lambert, A., Manney, G. L., Neu, J. L., Pitts, M. C., Werner, F., Livesey, N. J., and Schwartz, M. J.: The Evolution of the Hunga Hydration in a Moistening Stratosphere, Geophysical Research Letters, 51, e2024GL110 841, https://doi.org/https://doi.org/10.1029/2024GL110841, 2024.

Mote, P. W., Rosenlof, K. H., McIntyre, M. E., Carr, E. S., Gille, J. C., Holton, J. R., Kinnersley, J. S., Pumphrey, H. C., Russell III, J. M., and Waters, J. W.: An atmospheric tape recorder: The imprint of tropical tropopause temperatures on stratospheric water vapor, Journal of Geophysical Research: Atmospheres, 101, 3989–4006, https://doi.org/https://doi.org/10.1029/95JD03422, 1996.

Nedoluha, G. E., Gomez, R. M., Boyd, I., Neal, H., Allen, D. R., and Lambert, A.: The Spread of the Hunga Tonga H2O Plume in the Middle Atmosphere Over the First Two Years Since Eruption, Journal of Geophysical Research: Atmospheres, 129, e2024JD040 907, https://doi.org/https://doi.org/10.1029/2024JD040907, 2024.

https://doi.org/10.5194/egusphere-2026-4022
Preprint. Discussion started: 6 August 2026

Nicolet, M.: The photodissociation of water vapor in the mesosphere, Journal of Geophysical Research: Oceans, 86, 5203–5208, https://doi.org/https://doi.org/10.1029/JC086iC06p05203, 1981.

Niemeier, U., Wallis, S., Timmreck, C., van Pham, T., and von Savigny, C.: How the Hunga Tonga—Hunga Ha'apai Water Vapor Cloud Impacts Its Transport Through the Stratosphere: Dynamical and Radiative Effects, Geophysical Research Letters, 50, e2023GL106 482, https://doi.org/https://doi.org/10.1029/2023GL106482, 2023.

Peng, Y., Randel, W., Toon, O., Wang, X., Qie, K., Davis, S., Rosenlof, K., and Yu, P.: Moderate Volcanic Eruptions and Extreme Wildfires Humidify the Stratosphere, Nature, https://doi.org/https://doi.org/10.1038/s41586-026-10731-0, 2026.

Plumb, R. A.: Stratospheric transport, Journal of the Meteorological Society of Japan. Ser. II, 80, 793–809, https://doi.org/https://doi.org/10.2151/jmsj.80.793, 2002.

Proud, S. R., Prata, A. T., and Schmauß, S.: The January 2022 eruption of Hunga Tonga-Hunga Ha'apai volcano reached the mesosphere, Science, 378, 554–557, https://doi.org/10.1126/science.abo4076, 2022.

Randel, W. and Park, M.: Diagnosing Observed Stratospheric Water Vapor Relationships to the Cold Point Tropical Tropopause, Journal of Geophysical Research: Atmospheres, 124, 7018–7033, https://doi.org/https://doi.org/10.1029/2019JD030648, 2019.

Randel, W. and Starr, J.: RO Climate Data Record, https://www.cosmic.ucar.edu/RO_Climate_Data_Record, accessed: 2026-02-03, 2026.

Randel, W. J., Podglajen, A., and Wu, F.: Stratospheric Transit Time Distributions Derived From Satellite Water Vapor Measurements, Journal of Geophysical Research: Atmospheres, 129, e2024JD041 595, https://doi.org/https://doi.org/10.1029/2024JD041595, 2024.

Santee, M. L., Lambert, A., Froidevaux, L., Manney, G. L., Schwartz, M. J., Millán, L. F., Livesey, N. J., Read, W. G., Werner, F., and Fuller, R. A.: Strong Evidence of Heterogeneous Processing on Stratospheric Sulfate Aerosol in the Extrapolar Southern Hemisphere Following the 2022 Hunga Tonga-Hunga Ha'apai Eruption, Journal of Geophysical Research: Atmospheres, 128, e2023JD039 169, https://doi.org/https://doi.org/10.1029/2023JD039169, 2023.

Santee, M. L., Manney, G. L., Lambert, A., Millán, L. F., Livesey, N. J., Pitts, M. C., Froidevaux, L., Read, W. G., and Fuller, R. A.: The Influence of Stratospheric Hydration From the Hunga Eruption on Chemical Processing in the 2023 Antarctic Vortex, Journal of Geophysical Research: Atmospheres, 129, e2023JD040 687, https://doi.org/https://doi.org/10.1029/2023JD040687, 2024.

Schoeberl, M. R., Wang, Y., Ueyama, R., Taha, G., and Yu, W.: The Cross Equatorial Transport of the Hunga Tonga-Hunga Ha'apai Eruption Plume, Geophysical Research Letters, 50, e2022GL102 443, https://doi.org/https://doi.org/10.1029/2022GL102443, 2023.

Schoeberl, M. R., Toohey, M., Wang, Y., and Ueyama, R.: Stratospheric Injection Lifetimes, Journal of Geophysical Research: Atmospheres, 130, e2025JD043 928, https://doi.org/https://doi.org/10.1029/2025JD043928, 2025.

Sheese, P. E., Boone, C. D., and Walker, K. A.: Detecting physically unrealistic outliers in ACE-FTS atmospheric measurements, Atmospheric Measurement Techniques, 8, 741–750, https://doi.org/10.5194/amt-8-741-2015, 2015.

Sheese, P. E., Walker, K. A., Boone, C. D., Bernath, P. F., Froidevaux, L., Funke, B., Raspollini, P., and von Clarmann, T.: ACE-FTS ozone, water vapour, nitrous oxide, nitric acid, and carbon monoxide profile comparisons with MIPAS and MLS, Journal of Quantitative Spectroscopy and Radiative Transfer, 186, 63–80, https://doi.org/https://doi.org/10.1016/j.jqsrt.2016.06.026, satellite Remote Sensing and Spectroscopy: Joint ACE-Odin Meeting, October 2015, 2017.

Solomon, S., Rosenlof, K. H., Portmann, R. W., Daniel, J. S., Davis, S. M., Sanford, T. J., and Plattner, G.-K.: Contributions of Stratospheric Water Vapor to Decadal Changes in the Rate of Global Warming, Science, 327, 1219–1223, https://doi.org/10.1126/science.1182488, 2010.

Stocker, M., Steiner, A. K., Ladstädter, F., Foelsche, U., and Randel, W. J.: Strong persistent cooling of the stratosphere after the Hunga eruption, Communications Earth & Environment, 5, 450, https://doi.org/https://doi.org/10.1038/s43247-024-01620-3, 2024.

Toohey, M., Jia, Y., Khanal, S., and Tegtmeier, S.: Stratospheric residence time and the lifetime of volcanic stratospheric aerosols, Atmospheric Chemistry and Physics, 25, 3821–3839, https://doi.org/10.5194/acp-25-3821-2025, 2025.

Vömel, H., Oltmans, S. J., Hofmann, D. J., Deshler, T., and Rosen, J. M.: The evolution of the dehydration in the Antarctic stratospheric vortex, Journal of Geophysical Research: Atmospheres, 100, 13 919–13 926, https://doi.org/https://doi.org/10.1029/95JD01000, 1995.

Vömel, H., Rummukainen, M., Kivi, R., Karhu, J., Turunen, T., Kyrö, E., Rosen, J., Kjome, N., and Oltmans, S.: Dehydration and sedimentation of ice particles in the Arctic stratospheric vortex, Geophysical Research Letters, 24, 795–798, https://doi.org/https://doi.org/10.1029/97GL00668, 1997.

Wang, X., Randel, W., Zhu, Y., Tilmes, S., Starr, J., Yu, W., Garcia, R., Toon, O. B., Park, M., Kinnison, D., Zhang, J., Bourassa, A., Rieger, L., Warnock, T., and Li, J.: Stratospheric Climate Anomalies and Ozone Loss Caused by the Hunga Tonga-Hunga Ha'apai Volcanic Eruption, Journal of Geophysical Research: Atmospheres, 128, e2023JD039 480, https://doi.org/https://doi.org/10.1029/2023JD039480, 2023.

Waters, J., Froidevaux, L., Harwood, R., Jarnot, R., Pickett, H., Read, W., Siegel, P., Cofield, R., Filipiak, M., Flower, D., Holden, J., Lau, G., Livesey, N., Manney, G., Pumphrey, H., Santee, M., Wu, D., Cuddy, D., Lay, R., Loo, M., Perun, V., Schwartz, M., Stek, P., Thurstans, R., Boyles, M., Chandra, K., Chavez, M., Chen, G.-S., Chudasama, B., Dodge, R., Fuller, R., Girard, M., Jiang, J., Jiang, Y., Knosp, B., LaBelle, R., Lam, J., Lee, K., Miller, D., Oswald, J., Patel, N., Pukala, D., Quintero, O., Scaff, D., Van Snyder, W., Tope, M., Wagner, P., and Walch, M.: The Earth Observing System Microwave Limb Sounder (EOS MLS) on the Aura Satellite, IEEE Transactions on Geoscience and Remote Sensing, 44, 1075–1092, https://doi.org/10.1109/TGRS.2006.873771, 2006.

WMO: Meteorology – A three-dimensional science: Second session of the Commission for Aerology, WMO Bulletin, VI, 134–138, 1957.

Zhang, J., Kinnison, D., Zhu, Y., Wang, X., Tilmes, S., Dubé, K., and Randel, W.: Chemistry Contribution to Stratospheric Ozone Depletion After the Unprecedented Water-Rich Hunga Tonga Eruption, Geophysical Research Letters, 51, e2023GL105 762, https://doi.org/https://doi.org/10.1029/2023GL105762, 2024a.

Zhang, J., Wang, P., Kinnison, D., Solomon, S., Guan, J., Stone, K., and Zhu, Y.: Stratospheric Chlorine Processing After the Unprecedented Hunga Tonga Eruption, Geophysical Research Letters, 51, e2024GL108 649, https://doi.org/https://doi.org/10.1029/2024GL108649, 2024b.

Zhou, X., Dhomse, S. S., Feng, W., Mann, G., Heddell, S., Pumphrey, H., Kerridge, B. J., Latter, B., Siddans, R., Ventress, L., Querel, R., Smale, P., Asher, E., Hall, E. G., Bekki, S., and Chipperfield, M. P.: Antarctic Vortex Dehydration in 2023 as a Substantial Removal Pathway for Hunga Tonga-Hunga Ha'apai Water Vapor, Geophysical Research Letters, 51, e2023GL107 630, https://doi.org/https://doi.org/10.1029/2023GL107630, 2024.

Zhou, X., Chen, Q., Feng, W., Heddell, S., Dhomse, S. S., Mann, G., Pumphrey, H. C., Millán, L., Santee, M. L., and Chipperfield, M. P.: Residence time of Hunga stratospheric water vapour perturbation quantified at 9 years, Communications Earth & Environment, 7, https://doi.org/https://doi.org/10.1038/s43247-026-03216-5, 2026.

Zhu, Y., Bardeen, C. G., Tilmes, S., Mills, M. J., Wang, X., Harvey, V. L., Taha, G., Kinnison, D., Portmann, R. W., Yu, P., et al.: Perturbations in stratospheric aerosol evolution due to the water-rich plume of the 2022 Hunga-Tonga eruption, Communications Earth & Environment, 3, 248, https://doi.org/https://doi.org/10.1038/s43247-022-00580-w, 2022.

Zhu, Y., Akiyoshi, H., Aquila, V., Asher, E., Bednarz, E. M., Bekki, S., Brühl, C., Butler, A. H., Case, P., Chabrillat, S., Chiodo, G., Clyne, M., Colarco, P. R., Dhomse, S., Falletti, L., Fleming, E., Johnson, B., Jörimann, A., Kovilakam, M., Koren, G., Kuchar, A., Lebas, N., Liang, Q., Liu, C.-C., Mann, G., Manyin, M., Marchand, M., Morgenstern, O., Newman, P., Oman, L. D., Østerstrøm, F. F., Peng, Y., Plummer, D., Quaglia, I., Randel, W., Rémy, S., Sekiya, T., Steenrod, S., Sukhodolov, T., Tilmes, S., Tsigaridis, K., Ueyama, R., Visioni,

https://doi.org/10.5194/egusphere-2026-4022
Preprint. Discussion started: 6 August 2026

D., Wang, X., Watanabe, S., Yamashita, Y., Yu, P., Yu, W., Zhang, J., and Zhuo, Z.: Hunga Tonga–Hunga Ha'apai Volcano Impact Model Observation Comparison (HTHH-MOC) project: experiment protocol and model descriptions, Geoscientific Model Development, 18, 5487–5512, https://doi.org/10.5194/gmd-18-5487-2025, 2025.

Zhuo, Z., Wang, X., Zhu, Y., Yu, W., Bednarz, E. M., Fleming, E., Colarco, P. R., Watanabe, S., Plummer, D., Stenchikov, G., Randel, W., Bourassa, A., Aquila, V., Sekiya, T., Schoeberl, M. R., Tilmes, S., Zhang, J., Kushner, P. J., and Pausata, F. S. R.: Comparing multi-model ensemble simulations with observations and decadal projections of upper atmospheric variations following the Hunga eruption, Atmospheric Chemistry and Physics, 25, 13 161–13 176, https://doi.org/10.5194/acp-25-13161-2025, 2025.